Steady State Instability and Oscillation in Simplified Models of Tropospheric Chemistry

Mark R. Tinsley and Richard J. Field*

Department of Chemistry, The University of Montana, Missoula, Montana 59812

Received: February 14, 2001; In Final Form: September 25, 2001

Three components have been identified as being common to oscillation in five related but increasingly complex models of tropospheric chemistry. The first of these components is an NO_x-empty/refill cycle in which $[NO_x]$ grows or declines, depending upon the relative source rates of NO_x and HO_x, the latter being generally proportional to the rate of photolysis of $[O_3]$. The second component is a complex O_3-production/loss cycle dependent upon $[NO_x]$, $[HO_x]$, [CO], and $[O_3]$. The third component is nonlinear coupling (both direct and indirect) of the first two, which allows each of the two cycles to affect the other. This coupling also introduces a positive feedback that autocatalytically accelerates O_3 production at high [CO] and $[O_3]$ when $[NO_x]$ and $[NO]/[NO_2]$ are simultaneously low, thus destabilizing the steady state. A schematic model is provided that illustrates the interaction of these three components and indicates that the positive feedback indeed is necessary for oscillation to occur. The major features governing the behavior of this dynamic instability and related oscillation in simpler models also are dominant in a larger oscillatory model of tropospheric CH_4 photooxidation. Thus dynamical instability and oscillation appear to be common features of tropospheric chemical mechanisms, regardless of the particular reaction set chosen and over significant ranges of parameter values, and appear to result from complex nonlinear coupling of NO_x-empty/refill and O_3-production/loss cycles.

1. Introduction

Dynamical systems whose governing equation contains nonlinear terms as well as positive and negative feedback cycles may exhibit complex behavior including multiple steady states, excitability, steady-state instability, self-oscillation, and deterministic chaos.[1−5] Well known chemical examples are the Belousov−Zhabotinsky[2] and ClO_2^--based batch and continuous-flow stirred tank reactor (CSTR) oscillatory systems.[4] Recently,[6,7] mechanisms describing homogeneous tropospheric photochemistry also have been found to have such nonlinear, cyclic structure and to sometimes exhibit these behaviors in both simplified models[8−12] such as discussed here, as well as in much larger and more realistic representations of tropospheric chemistry.[7,11,13]

Much of this work has used well-mixed box models (essentially CSTRs) with simplified photochemistry composed of various subsets of a core of representative tropospheric reactions usually involving only the six variable concentrations: [CO], $[O_3]$, [NO], $[NO_2]$, [HO], and $[HO_2]$, together with various input and loss terms for NO, CO, and O_3, and a constant solar light flux. The species CO (representative of the class of volatile organic compounds, VOCs), O_3, NO, and NO_2 are significant trace-gas tropospheric pollutants, while the radicals HO and HO_2 are the engines of tropospheric photochemistry.

The major phenomena observed so far springing from the nonlinear dynamic structure of both small and large tropospheric models are multiple steady states, steady-state instability, limit cycle oscillation, and chaos. Tropospheric multiple steady states[8,14−16] are characterized by high or low values of $[NO_x] = [NO] + [NO_2]$ associated, respectively, with low and high values of $[HO_x] = [HO] + [HO_2]$. The oscillatory systems pass through similar states with simultaneous cycling of [CO] and $[O_3]$, although true multiple steady states are not necessary for the appearance of oscillation.[17] The identification of high and low-$[NO_x]$ states is of considerable practical utility, especially in the interpretation of heavily polluted real tropospheric states.[18−20] These oscillations are intrinsic to the photochemistry itself; they are not driven by the diurnal solar cycle, as is the case in existing oscillatory models of upper-atmosphere chemistry.[21−23] Addition of the diurnal cycle into the present models leads only to the introduction of a ripple on the longer-period chemical oscillations,[10] although its amplitude is sometimes amplified near a bifurcation in models containing nighttime chemistry.[24]

The simulated oscillatory periods found so far range from the order of several weeks to centuries. Thus, it is unlikely that full cycles of even the shortest of these oscillations can be observed in any real, localized atmosphere necessarily subject to meteorological mixing on much shorter time scales. However, phases of sudden concentration change occur during these oscillations on time scales of 2−3 days, even in these relatively slow models. We do suggest that favorable places to observe evidence of these oscillations might include the summer polar troposphere, especially the boundary layer, when there is a strong 24-hour solar input,[25] and during stagnant summer high-pressure episodes in a high-altitude, low-latitude, heavily polluted tropospheric air mass such as is often found over Mexico City.[26]

On the other hand, it can be speculated that the very long oscillatory periods observed in these tropospheric models might, in a global troposphere that is well mixed on long time scales, couple with oceanic and biospheric forces, contributing to periodic climate variability[27] on the longer time scales observed in these models.

The potentially most significant phenomenon here is steady state instability; i.e., there may be no stable steady state toward which chemical concentrations must inevitably evolve. This suggests that the temporal evolution of tropospheric chemistry may sometimes be very sensitive to initial conditions, as well as to perturbation.[28] Thus, short term changes in chemical composition, perhaps previously ascribed to meteorology, may sometimes result instead from dynamic instability of the chemistry itself. To our knowledge, the implication of this instability for large models of tropospheric chemistry has yet to be carefully considered.[29]

Investigation of oscillation in simplified tropospheric models not only elucidates questions concerning steady state instability but also clarifies the basic nonlinear structure of tropospheric

10.1021/jp010571t CCC: $20.00
Published on Web 11/17/2001

chemical dynamics, especially the shifting balance between growth and loss of tropospheric [NO_x], [HO_x], and [VOCs] (CSTR empty/refill processes) resulting from their nonlinear coupling to the chemistry initiated by the photolysis of O_3 in the presence of VOCs. The fingerprints of relative concentration changes of various species resulting from motion near to the steady state in these models may well be useful in identifying chemical instability in a real atmosphere.

We consider here four simplified tropospheric models exhibiting steady state instability and oscillation and find that while there are significant differences among them, the basic interactions leading to these phenomena are very similar.

2. Simplified Tropospheric Models

The core model here is that of Field et al.,[6] referred to as model M1.

$$O_3 + h\nu \xrightarrow{H_2O} 2HO \qquad k_1 = 6.9 \times 10^{-8} \qquad \text{(R1)}$$

$$CO + HO \xrightarrow{O_2} HO_2 + CO_2 \qquad k_2 = 1.9 \times 10^{-13} \qquad \text{(R2)}$$

$$HO_2 + O_3 \rightarrow HO + 2O_2 \qquad k_3 = 1.5 \times 10^{-15} \qquad \text{(R3)}$$

$$NO + O_3 \rightarrow NO_2 + O_2 \qquad k_4 = 7.9 \times 10^{-15} \qquad \text{(R4)}$$

$$NO_2 + h\nu \xrightarrow{O_2} NO + O_3 \qquad k_5 = 3.9 \times 10^{-3} \qquad \text{(R5)}$$

$$HO_2 + NO \rightarrow HO + NO_2 \qquad k_6 = 9.6 \times 10^{-12} \qquad \text{(R6)}$$

$$HO + NO_2 \rightarrow HNO_3 \qquad k_7 = 1.3 \times 10^{-11} \qquad \text{(R7)}$$

$$\rightarrow CO \qquad S_{CO} \text{ Table 1}$$

$$\rightarrow O_3 \qquad S_{O3} \text{ Table 1}$$

$$\rightarrow NO \qquad S_{NO} \text{ Table 1}$$

First-order (photolysis) reaction rate constants are given in s^{-1} and second-order rate constants are given in cm^3 molecule^{-1} s^{-1}. The concentrations of O_2, H_2O, and CO_2 are assumed to be constant. Details of the choice of rate parameter values are given in Hess and Madronich[11] and Field et al.[6] The absence of physical-loss and radical-recombination terms (a radical species is defined here following Kleinman[14] as a member of the odd-hydrogen family and hydrocarbon analogues, e.g., HO, HO_2, RO_2, etc.) in this, the simplest model discussed here, emphasizes the balance of influx of NO and CO with their photochemical removal. This model shows[6] a subcritical Hopf bifurcation to an unstable steady state and associated evolution to limit cycle oscillation as S_{NO} is increased with the values of all other parameters held constant. It undergoes a period-doubling transition to deterministic chaos at still higher S_{NO}. The other models considered here are obtained by adding dynamic processes to this core.

Model M2 is obtained by addition to M1 of the two processes below.

$$HO_2 + HO_2 \rightarrow H_2O_2 + O_2 \qquad k_8 = 2.9 \times 10^{-12} \qquad \text{(R8)}$$

$$NO \rightarrow L_{NO} \quad \text{Table 1}$$

It exhibits an unstable steady state and oscillation but not chaos for the parameters used here.

TABLE 1: Source and Loss Terms for Models M1−M4[a]

parameter	M1	M2	M3	M4
S_{CO}	5.0×10^5	5.0×10^5	5.0×10^5	5.0×10^6
S_{O3}	6.0×10^4	6.0×10^4	6.0×10^4	6.0×10^4
S_{NO}	5.0×10^4	3.0×10^5	3.0×10^5	3.0×10^6
L_{NO}		5.0×10^{-6}	5.0×10^{-6}	2.3×10^{-8}

[a] Source terms (S_{CO}, S_{O3}, and S_{NO}) are given in molecule cm^{-3} s^{-1}. Loss terms (L_{NO}) are given in s^{-1}.

Model M3 is similar to that used by Krol and Poppe[12] and is obtained by adding reaction R9 to M2.

$$HO + O_3 \rightarrow HO_2 + O_2 \qquad k_9 = 7.0 \times 10^{-14} \qquad \text{(R9)}$$

Model M3 also exhibits an unstable steady state and oscillation but not chaos.

Model M4 is based upon that of Stewart[8] and is obtained by adding reaction R10 to M3 in order to extend the model to include hydrocarbon oxidation.

$$CH_4 + HO \rightarrow CO + 2HO_2 \qquad k_{10} = 6.5 \times 10^{-15} \qquad \text{(R10)}$$

Reaction R10 represents a complex sequence of elementary processes and is the only stoichiometrically autocatalytic reaction present in M1−M4, yielding two HO_x species from one. Crutzen[30] suggests a similar autocatalysis that occurs only at high [NO_x], a subtlety not present in this formulation of R10. The [CH_4] is kept fixed at 4.2×10^{13} molecules/cm^3 in M4, which exhibits oscillation but not chaos. It is the only model used here for which true multiple steady states have been located.

The rate constant values specified above are well established[6] and used in all models. However, it is necessary in order to obtain steady state instability and oscillation to use somewhat different values in each model for the source and loss terms for CO, NO, and O_3. These parameters are in fact quite variable in natural atmospheres. Table 1 shows the values of these parameters used in each model.

Typical oscillations in [CO], [O_3], [NO_x], and [HO_x] are shown in Figure 1 for models M1−M4. Simultaneous values of the ratios [NO]/[NO_2] and [HO]/[HO_2] are shown in Figure 2. Certain features common to all four models emerge from examination of these traces. (1) Each oscillation consists of a region of higher [NO_x] (with corresponding lower [HO_x]), during which both [CO] and [O_3] increase, with the rate of O_3 production gradually accelerating through the region. (2) This higher [NO_x] region is followed by a lower [NO_x] region (with corresponding higher [HO_x]), during which both [CO] and [O_3] decrease. (3) Transition from the higher [NO_x] region to the lower [NO_x] region is relatively rapid. It is accompanied by an initial sharp acceleration in O_3 production followed by sometimes quite rapid O_3 consumption, as well as by declining [CO] and large decreases in the ratios [NO]/[NO_2] and [HO]/[HO_2]. This initial sharp acceleration in O_3 production is of particular importance to the following analysis and is highlighted in Figure 1 by an arrow. (4) Transition from the lower [NO_x] region to the higher [NO_x] region also is relatively rapid and leads to completion of the cycle. It signals the onset of relatively slow growth in [O_3] and [CO], as well as rapid growth in [NO]/[NO_2] and [HO]/[HO_2].

On this basis, it is useful to break the oscillations and their analysis into three key common components. (1) NO_x empty/refill, (2) O_3 production/loss, and (3) chemical coupling/feedback. While these three components are intimately linked, occurring simultaneously, it is instructive to discuss each

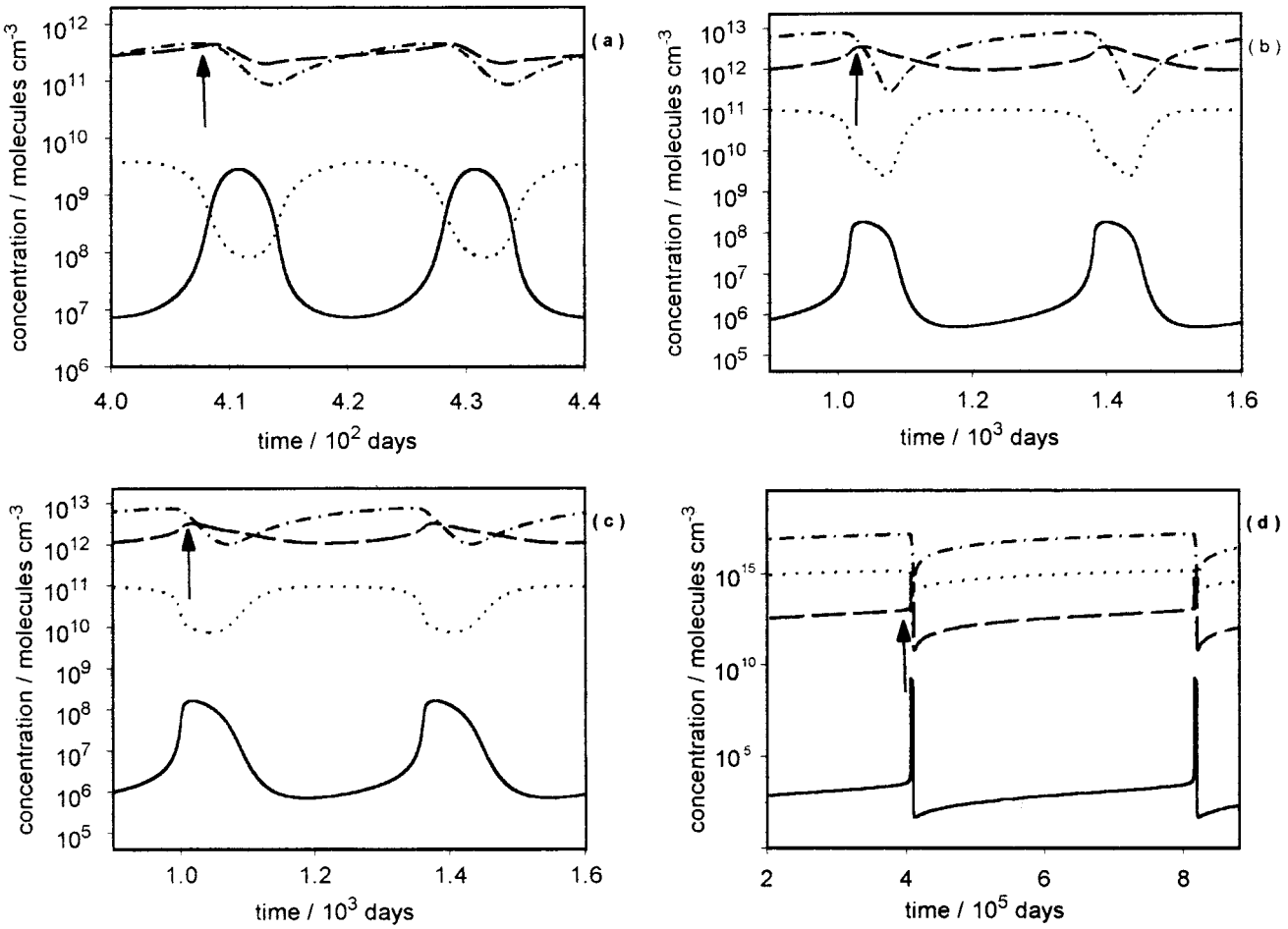

Figure 1. Oscillation versus time (days) of the logarithmic concentrations (molecule cm^{-3}) of HO_x (solid line), NO_x (dotted line), O_3 (dashed line), and CO (dash−dotted line) for models M1−M4, a−d, respectively. The arrow indicates accelerated O_3 production as discussed in the text.

separately. The following is applicable to all four models, M1−M4. Model M2 is used to demonstrate discussion points.

3. NO_x Empty/Refill

Systems M1−M4 fill with NO_x via net physical influx of NO, i.e., $E_{NOx} = S_{NO} - L_{NO}[NO]$. They empty of NO_x via chemical reaction. Both NO_x species, NO and NO_2, contain an unpaired electron and may combine with radical species (R), e.g., HO or CH_3COO_2, usually to yield a relatively stable molecule. We write this process as R11.

$$NO_x + R \rightarrow RNO_x \qquad \text{(R11)}$$

This process is a sink of both radicals and NO_x because the product species (RNO_x) usually are either relatively unreactive or removed from the troposphere by physical deposition processes. The only reaction of this type in models M1−M4 is R7. A tropospheric system is sometimes considered[16] to be in a high [NO_x] state when

$$E_R \ll E_{NOx} \qquad (1)$$

where E_R is the net rate of radical production. Excess NO_x influx under this condition rapidly titrates (stoichiometrically removes) radicals in R11, leading to low radical concentrations while [NO_x] grows. However, if

$$E_R \gg E_{NOx} \qquad (2)$$

then the system sometimes is considered to be in a low [NO_x] state because excess radical production now titrates NO_x, leading to declining [NO_x], and higher radical concentrations where combination/disproportionation reactions, e.g., R8, may become a significant added sink for radical species. These ideas due to Kleinmann[14,16] provide a useful framework for understanding tropospheric chemical oscillation.

The rate of radical entry for M1−M3 is given by $E_R = 2R_{R1}$ and for M4 by $E_R = 2R_{R1} + R_{R10}$, where R_{R1}, etc. are the rates of the corresponding reactions. The net influx of NO_x is given by $S_{NOx} - L_{NO}[NO]$. The value of [NO_x] generally increases when $E_R - E_{NOx} < 0$ and decreases when $E_R - E_{NOx} > 0$, as is shown in Figure 3 for two cycles of M2. Because [NO_x] is not always low when (1) is true, we refer to this as the region of decreasing rather than of low [NO_x]. Similarly when (2) is true we refer to this as the region of increasing rather than of high [NO_x]. These regions of decreasing and increasing [NO_x] give rise to the concept of NO_x empty/refill.

The behavior of [HO_x] is inversely correlated to that of [NO_x]. In general, when the system is filling with NO_x, then [HO_x] is declining, and vice versa. An exception to this behavior may occur toward the end of the NO_x-emptying region if radical−radical recombination reactions become a significant radical-loss process.

Therefore, oscillation in models M1−M4 may be viewed as a switching between increasing and decreasing [NO_x] regimes that is driven by variable relative rates of radical production, E_R, as compared to E_{NOx}. Radical production in M1−M4 occurs mainly through O_3 photolysis in R1, and thus is strongly dependent upon [O_3], whose behavior in turn is strongly

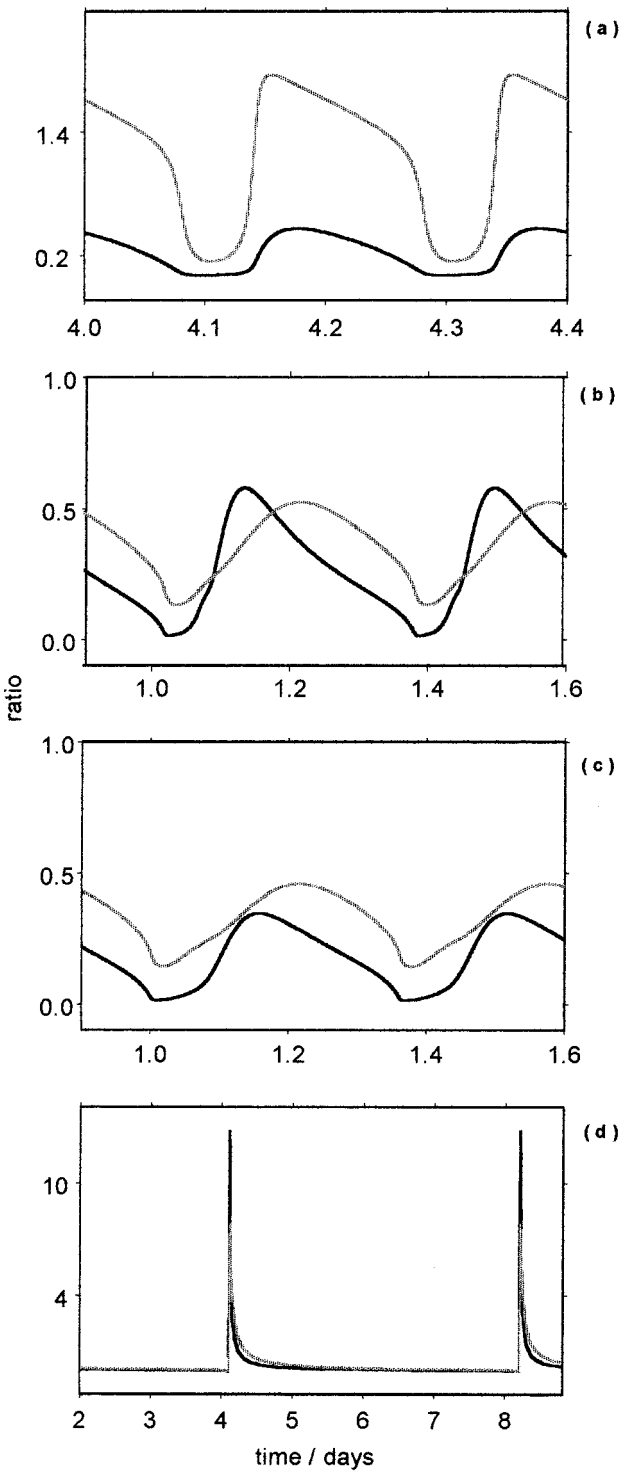

Figure 2. Oscillation versus time (days) of the ratios [HO]/[HO_2] (solid line) and [NO]/[NO_2] (gray line) for models M1−M4, a−d, respectively. The time-axis scalings are as in Figure 1.

dependent upon [NO_x] and [NO]/[NO_2], introducing significant feedback coupling into the system. The processes controlling [O_3] are discussed next.

4. Ozone Production and Loss Cycles

The oxidation of trace gases (e.g., VOCs and NO) in the troposphere is initiated primarily by HO radical, whose major source is the photolysis of O_3. Thus, [O_3] determines both the oxidizing capacity of the troposphere, and through E_R, whether it is in an NO_x-filling or NO_x-emptying state. Ozone itself may

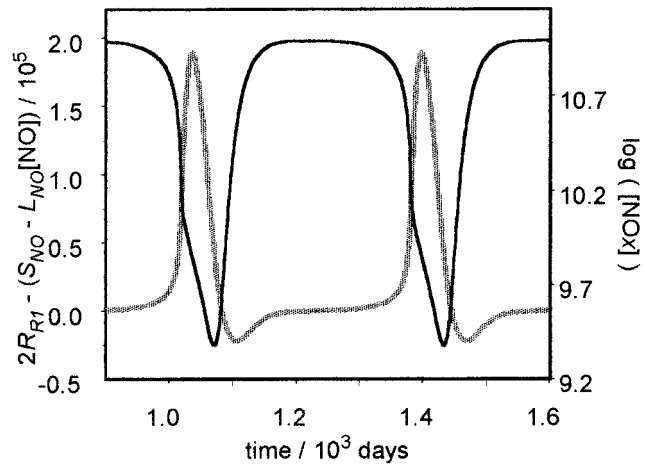

Figure 3. Oscillation versus time (days) of the difference between the source rates (molecule cm^{-3} s^{-1}) of radicals and of NO_x, $E_R - E_{NOx} = 2R_{R1} - (S_{NO} - L_{NO}[NO])$, in model M2 (gray line). Simultaneous oscillation of logarithmic [NO_x] (molecule cm^{-3}) (solid line).

be either created or destroyed in this oxidation process, depending upon the balance between various O_3-production and O_3-loss cycles.

Field et al.[6] discuss the O_3-production and O_3-loss cycles in M1 in some detail. A modification of their O_3-production cycle is given below.

$$CO + HO \xrightarrow{O_2} HO_2 + CO_2 \qquad (R2)$$

$$NO + HO_2 \rightarrow NO_2 + HO \qquad (R6)$$

$$NO + O_3 \rightarrow NO_2 + O_2 \qquad (R4)$$

$$NO_2 + h\nu \xrightarrow{O_2} O_3 + NO \qquad (R5)$$

$$CO + h\nu \xrightarrow{2O_2} CO_2 + O_3 \qquad (S1)$$

Stoichiometry S1 assumes that $R_{R6} > R_{R4}$ during O_3 production, allowing R_{R4} to be ignored in forming S1.

This production cycle differs from that of Field et al.[6] and others[31] by the presence of reaction R4, which is included here because the [NO]/[NO_2]-mediated rate difference ($R_{R5} - R_{R4}$) is a better measure of the net rate of O_3 formation in S1 than is either R_{R5} or R_{R4} alone. Indeed, the quantity ($R_{R5} - R_{R4}$) is sufficiently important for the present analysis to be defined as F_{O3}, which may be either positive or negative, and thus contribute to either net O_3 production or net O_3 loss. The efficiency of O_3 production in S1 per photochemically generated HO may be defined by the quantity $(R_{R5} - R_{R4})/2R_{R1}$, which is shown for model M2 in Figure 4. The acceleration of O_3 production indicated in Figure 4 by the sharp peaks near the end of the [O_3]-growth regime occurs at high [O_3]/[NO_2] and is discussed in the next section. At sufficiently high [O_3], $E_R > E_{NOx}$, and the system enters an [NO_x]-emptying state.

While the O_3-production cycle S1 is the same in all four models discussed here, the O_3-loss cycle is model dependent. Ozone loss becomes dominant over O_3 production as [O_3] grows and [NO_x] declines due to changes in a combination of factors: (1) increasing [HO_x] and [O_3], leading to enhanced loss of O_3 via $HO_x + O_3$ reactions, e.g., R3 and R9; (2) increasing [O_3], leading to increased absolute rate of O_3 destruction via photolysis, R1, which becomes important when O_3-formation processes slow; and (3) changes in F_{O3} resulting from changes in [O_3], [NO_x], and [NO]/[NO_2].

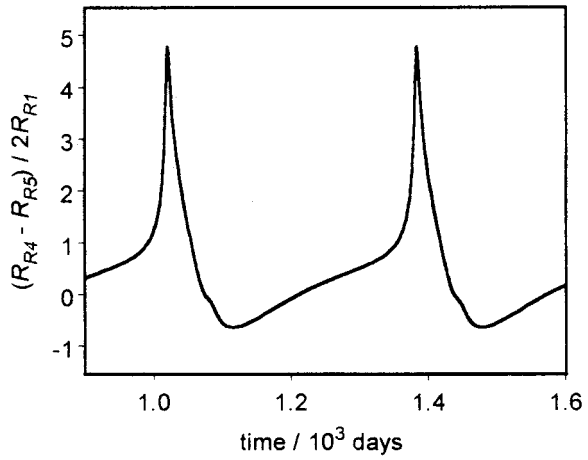

Figure 4. Photochemical efficiency (dimensionless) of the O_3-production cycle S1 versus time (days) as given by the quantity $F_{O3}/2R_{R1} = (R_{R5} - R_{R4})/2R_{R1}$ during oscillation of model M2.

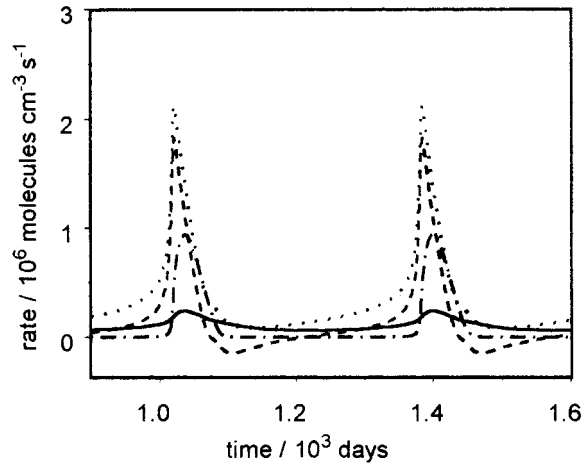

Figure 5. Key reaction rates (molecule cm^{-3} s^{-1}) contributing to the transition from O_3 production to O_3 loss versus time (days) during oscillation of model M2. R_{R1} (solid line), R_{R3} (dash-dotted line), R_{R6} (dotted line), and $F_{O3} = (R_{R5} - R_{R4})$ (dashed line).

The change from net O_3 production to net O_3 loss at low [NO_x] is illustrated in Figure 5 using various reaction rates for model M2. Toward the end of the O_3-production region, NO_x-mediated O_3 production in S1 via F_{O3} is slowed as [NO_2] declines. Ozone loss through both reaction with HO_2 (reaction R3) and photolysis (reaction R1) then leads to net O_3 loss. Depending upon the details of the particular model, F_{O3} itself may become negative in this region and contribute to O_3 loss. This decreasing [O_3] leads to a decrease in radical formation in R1 such that eventually the source rate of NO_x becomes greater than the source rate of radicals ($E_{NOx} - E_R > 0$), and the system switches to an [NO_x]-increasing regime, during which O_3 production must inevitably recover by the scenario below.

The transition from O_3 destruction to O_3 production with increasing [NO_x] also is complex and model dependent, with the same key factors present as in the transition from O_3 production to O_3 destruction, but in the opposite direction: (1) declining [HO_x] resulting from increasing [NO_x] reduces the loss of O_3 via reaction with HO_x; (2) declining [O_3] reduces the loss of O_3 via photolysis; (3) changes in F_{O3}, (a) increasing [NO_x] and decreasing [O_3] cause F_{O3} to increase and (b) during this period [NO]/[NO_2] also may change from increasing to decreasing (pass through a maximum), leading to increased F_{O3}.

Model M2 is used to demonstrate this behavior. Near to the turning point from net O_3 loss to net O_3 production, destruction of O_3 by HO_2 falls to nearly zero. The O_3-destruction capacity of F_{O3} is reduced due to decreasing [O_3]. The [O_3] turning point coincides with the maximum in [NO]/[NO_2], beyond which decreasing [NO]/[NO_2] leads to increased O_3 formation in F_{O3}. (The ratio [NO]/[NO_2] is determined by loss of NO via linear deposition, L_{NO}, NO_2 loss via reaction with HO, R7, and by the rate of interconversion of NO and NO_2 discussed in section 5.)

It may thus be seen that transitions between O_3 production and O_3 loss are dependent upon both cycling [HO_x] and [NO_x], which themselves are dependent upon the cycling [O_3]. The coupling between these two cycles is described in the next section.

5. Chemical Feedback

The final important feature of these oscillations is coupling of the O_3-production/loss and NO_x-empty/refill cycles. This coupling takes place in two key ways: directly through the F_{O3} term and indirectly through HO_x chemistry. It results in high-[NO_x] states necessarily evolving toward low-[NO_x] states (and vice versa), while dominance of O_3 production necessarily evolves toward dominance of O_3 loss (and vice versa).

Photolysis of O_3 during high-[NO_x] conditions contributes to the system entering an NO_x-emptying state (i.e., $E_R > E_{NOx}$), which eventually causes transition to O_3 loss due to decreasing [NO_x] and increasing [HO_x]. However, in the resulting low-[O_3] state, the system must enter an NO_x-filling state because $E_R < E_{NOx}$. The increasing [NO_x] (and low [HO_x]) that result then lead to evolution toward an O_3-production state. This complex global feedback is illustrated schematically below.

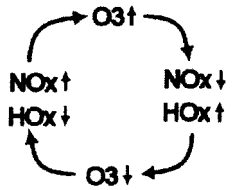

However, this enforced evolution of high-[NO_x] states toward low-[NO_x] states (and vice versa) and O_3-production states toward O_3-loss states (and vice versa) does not guarantee oscillation. Indeed, the effect of these forces might be an approach to an intermediate steady state. However, coupling of these two cycles also leads to creation of a subtle positive feedback loop operating throughout the O_3-production phase of an oscillation but becoming particularly strong near to its end. This results in a self-acceleration of the O_3-production rate, a phenomenon that has been described as autocatalysis by some authors.[3,4] This positive feedback loop apparently destabilizes the tropospheric chemical steady state under suitable conditions and leads to oscillation. It is described next.

Net O_3 production is controlled by the balance between the O_3-formation term, F_{O3}, and O_3-loss processes. Examination of these terms (e.g., the reaction rates in Figure 5) shows that the acceleration of O_3 production is associated with an increase in $(R_{R5} - R_{R4}) = F_{O3}$. During the period of acceleration, [O_3] is increasing but both [NO] and [NO_2] are decreasing. Therefore, the decreasing ratio [NO]/[NO_2] leads to increasing net O_3-production rate. (The explicit dependence of the quantity F_{O3} on [O_3], [NO_2], and [NO]/[NO_2] may be seen from the expression $F_{O3} = k_{R5}[NO_2] - k_{R4}[NO][O_3] = (k_{R5} - k_{R4}([NO]/[NO_2])[O_3])[NO_2]$.)

It is useful at this point to define the quantity C_N as the conversion rate of NO to NO_2. In M2, C_N is simply the signed

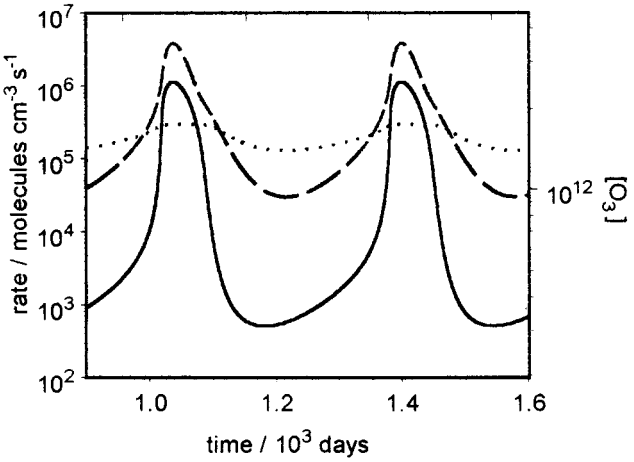

Figure 6. Logarithmic rates (molecule cm^{-3} s^{-1}) C_N (dotted line) and C_R (solid line) with logarithmic $[O_3]$ (molecule cm^{-3}) (dashed line) for reference versus time (days) during oscillation of model M2. The acceleration of O_3 production before the shift to O_3 loss is very apparent here.

sum, $R_{R4} - R_{R5} + R_{R6}$. Figure 5 displays these reaction rates for model M2, and Figure 6 displays C_N. When the system switches to a decreasing $[NO_x]$ state, $[HO_x]$ simultaneously increases according to the empty/refill processes described earlier. Initially, HO_x is formed as HO, but it is converted to HO_2 by CO in reaction R2. Loss of $[HO_x]$ via R7 also is diminished at higher $[CO]/[NO_2]$. The [CO] is high in the accelerated O_3-production phase of the cycle but beginning its rapid decline. The increasing $[HO_2]$ leads to an increase in C_N, which decreases $[NO]/[NO_2]$, leading to accelerated O_3 production and thus via O_3 photolysis to accelerated $[HO_x]$ production. This acceleration is critically dependent upon R2 and the presence of significant [CO]. It disappears as CO is rapidly consumed during this phase of the cycle. Thus, somewhat delayed depletion (emptying) of CO by increasing $[O_3]$ at this point is a critical feature of oscillation.

The conversion rate of HO to HO_2 may be measured by C_R, which for M2 is given by the difference between the rates of reactions R2 and R6 and is displayed in Figure 6. Reaction R3 is not important during the O_3-production stage. The quantity C_R is enhanced as [CO] increases and as [NO] decreases. Thus, $[HO_x]$ is increasingly in the form of HO_2 as the cycle evolves toward higher $[O_3]$ and [CO], which increases C_N, which in its turn decreases $[NO]/[NO_2]$. This overall positive feedback process is represented in the diagram below.

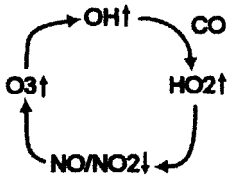

It does not seem possible to attribute a "prime cause" to this feedback process. Increasing $[O_3]$, increasing [HO] and $[HO_2]$, and decreasing $[NO]/[NO_2]$ occur simultaneously and reinforce each other as described above.

6. Methane Model

Application of the above ideas is straightforward to the more complex model of tropospheric CH_4 photooxidation shown in Table 2 (referred to as M5) and found to be oscillatory by Madronich et al.[32] This chemistry is extracted from the very large National Center for Atmospheric Research (NCAR) Master Mechanism[33] for tropospheric chemistry (which also exhibits steady-state instability and oscillation[7]) and involves 14 species and 29 reactions. Typical oscillations are shown in Figure 7 and have characteristics similar to those of models M1−M4, with $[CH_4]$ (which varies in this model in contrast to M4 where it is held constant) behaving similarly to [CO]. However, the long period and spiked nature of the oscillations are most similar to those of model M4.

This oscillation again may be explained in terms of NO_x-empty/refill coupled to O_3-production and loss cycles. Regions

TABLE 2: Mechanism of Tropospheric Photooxidation of CH_4 (model M5)

	reaction (sources, sinks, R1 − R9)[a]	rate constant[b]
(R12)	$HO + HO \rightarrow H_2O_2$	4.0×10^{-12}
(R13)	$2HO + O_2 \rightarrow O_3 + H_2O$	1.6×10^{-12}
(R14)	$HO + HO_2 \rightarrow H_2O + O_2$	1.3×10^{-10}
(R15)	$H_2 + HO \xrightarrow{O_2} HO_2 + H_2O$	2.0×10^{-15}
(R16)	$H_2O_2 \rightarrow 2HO$	3.1×10^{-6}
(R17)	$H_2O_2 + HO \rightarrow HO_2 + H_2O$	1.5×10^{-12}
(R18)	$CH_4 + HO \xrightarrow{O_2} CH_3O_2$	2.8×10^{-15}
(R19)	$CH_3O_2 + HO_2 \rightarrow CH_3OOH + O_2$	7.7×10^{-12}
(R20)	$2CH_3O_2 \rightarrow 2CH_2O + 2HO_2$	2.1×10^{-13}
(R21)	$2CH_3O_2 \rightarrow CH_2O + CH_3OH + O_2$	3.1×10^{-13}
(R22)	$CH_3OOH \xrightarrow{O_2} CH_2O + HO_2 + HO$	2.4×10^{-6}
(R23)	$CH_3OO + HO \rightarrow CH_3OO + H_2O$	5.8×10^{-12}
(R24)	$CH_3OOH + HO \rightarrow CH_2O + HO + H_2O$	2.5×10^{-12}
(R25)	$CH_3OH + HO \xrightarrow{O_2} CH_2O + HO_2$	6.2×10^{-13}
(R26)	$CH_2O \xrightarrow{2O_2} CO + 2HO_2$	1.2×10^{-5}
(R27)	$CH_2O \rightarrow CO + H_2$	1.9×10^{-5}
(R28)	$CH_2O + HO \xrightarrow{O_2} CO + HO_2 + H_2O$	1.0×10^{-11}
(R29)	$NO + CH_3(OO.) \rightarrow NO_2 + CH_2O + HO_2$	8.5×10^{12}
(R30)	$HNO_3 + h\nu \rightarrow HO + NO_2$	2.0×10^{-7}
(R31)	$HNO_3 + HO \rightarrow 0.89NO_2 + 0.89O_3 + 0.11NO$	2.6×10^{-13}

[a] Source rates (molecule cm^{-3} s^{-1}): $S_{O3} = 5.0 \times 10^4$, $S_{CH4} = 1.2 \times 10^5$, $S_{CO} = 2.1 \times 10^5$, $S_{NO} = 4.0 \times 10^3$. Loss (sink) rates (s^{-1}): $L_{HNO3} = 3.0 \times 10^{-}$,[6] $L_{H2O2} = L_{CH3OOH} = L_{CH2O} = 2.5 \times 10^{-}$,[6] $L_{NO2} = 7.2 \times 10^{-}$,[7] $L_{NO} = 1.9 \times 10^{-}$,[7] $L_{O3} = 9.6 \times 10^{-}$,[8] $L_{CO} = 3.2 \times 10^{-}$;[8] $L_{H2} = 1.4 \times 10^{-}$,[8] $L_{CH4} = 3.2 \times 10^{-10}$. Reactions R1−R9 and their rate parameters are given in text. [b] Rates calculated for equinox conditions, 5 km altitude at latitude 30° N, assuming $T = 253$ K, air density of 1.5×10^{19} molecules/cm^3 and 50% relative humidity. Rate coefficients are given in units of s^{-1} and cm^3 molecule^{-1} s^{-1} for first- and second-order reactions, respectively.

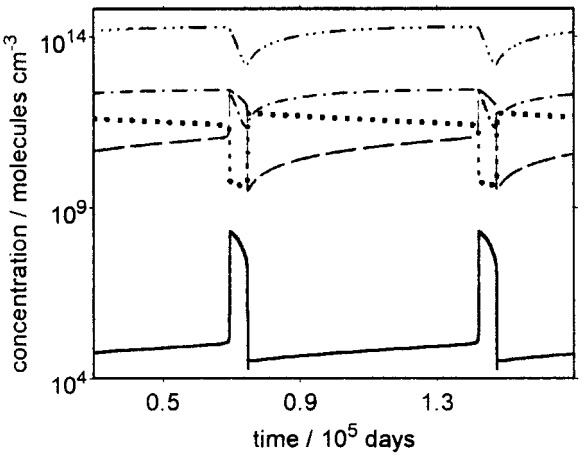

Figure 7. Logarithmic concentration (molecules cm^{-3}) oscillations versus time (days) in model M5 of CH_4 photooxidation. $[HO_x]$ (solid line), $[NO_x]$ (dotted line), $[O_3]$ (dashed line), [CO] (dashed-dotted line), and $[CH_4]$ (triple dotted-dashed line).

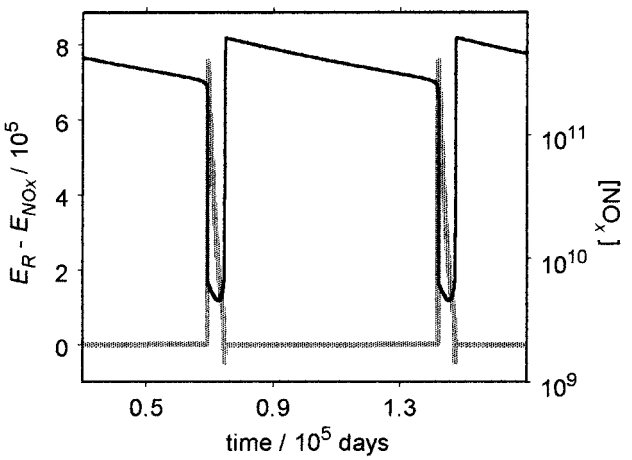

Figure 8. Oscillation of logarithmic [NO_x] (solid line) and the difference between the source rates (molecule cm^{-3} s^{-1}) of radicals ($E_R = 2R_{R1} + 2R_{R25}$) and of NO_x ($E_{NOx} = S_{NO} - L_{NO}[NO] - L_{NO2}[NO_2]$) (gray line) in model M5 of the photooxidation of CH_4.

of emptying and filling may be identified using equations (1) and (2). The radical source rate is given by $E_R = 2R_{R1} + 2R_{R26}$ and the net source rate of NO_x is given by $E_{NOx} = S_{NO} - L_{NO}[NO] - L_{NO2}[NO_2]$. Figure 8 shows the oscillatory values of $E_R - E_{NOx}$ and log [NO_x].

The [O_3]-formation rate, F_{O3}, again is defined as ($R_{R5} - R_{R4}$). Production of O_3 occurs via the same set of reactions as in models M1−M4, with the efficiency of O_3 production now being defined as $F_{O3}/(2R_{R1} + 2R_{R25})$. The switch from O_3 production to O_3 destruction again occurs due to a combination of the changing efficiency of F_{O3} and the increasing importance of $O_3 + HO_x$ destruction reactions. Ozone production again restarts via F_{O3} due to decreased [O_3] and [NO]/[NO_2].

Of particular interest here are the long oscillatory period and the extremely rapid acceleration of the O_3-production rate in M4 and M5. As was discussed in section 5 for model M4, these characteristics are due to a complex feedback process involving the conversion rates C_R and C_N. In model M4 they are *not* due to the stoichiometric autocatalysis reaction R10. Examination of the relative importance of reactions leading to the formation of HO_2 shows that R10 plays only a secondary role during the acceleration of O_3 production. The spiked nature and long period of the oscillation are instead created by the relative distribution of species involved in the O_3-production and acceleration (feedback) mechanisms. For example, during the increasing [NO_x] portion of the M4 oscillation, [HO_x] is very low and [CO] and [NO_x] are very high as compared to models M1−M3.

Similarly for M5, no evidence has been found for significant net stoichiometric autocatalysis during the acceleration of [O_3] production. The acceleration is due to the same feedback as in the other models. Increases in C_R and C_N with increasing [O_3] lead to decreasing [NO]/[NO_2], which results in increasing F_{O3}. Again [HO_x] is low during the increasing [NO_x] stage and total VOC ([CH_4] + [CO]) concentration is high. It has not yet been possible to determine for models M1−M5 quantitative relationships between species concentrations and either the oscillatory period or the O_3-acceleration rate, as was instructively done by Hess and Madronich[11] in a similar model.

7. A Schematic Model

Scheme N below has been developed to capture the essential features of the NO_x-empty/refill and O_3-production/loss cycles, and their coupling.

$$\rightarrow S_{O3} \quad \text{(N1)}$$

$$\rightarrow S_{NOx} \quad \text{(N2)}$$

$$O_3 \xrightarrow{k_{N1}} 2HO_x \quad \text{(N3)}$$

$$HO_x + NO_x \xrightarrow{k_{N2}} \quad \text{(N4)}$$

$$O_3 + HO_x \xrightarrow{k_{N3}} HO_x \quad \text{(N5)}$$

The dynamic variables in Scheme N are dimensionless [O_3], [NO_x], and [HO_x], while S_{O3}, S_{NOx}, and $k_{N1}-k_{N3}$ are parameters chosen to be of order one. Reactions N1 and N2 represent source (production/filling) terms for O_3 and NO_x, respectively. Reactions N3, N4, and N5 represent, respectively, photochemical HO_x generation from O_3, the NO_x and HO_x emptying process, and HO_x-catalyzed O_3 loss. Scheme N includes the basic O_3-production/loss and NO_x-empty/refill mechanisms but only indirect coupling of NO_x and O_3 chemistry via HO_x. Linear stability analysis of its mass-action dynamic equation shows that Scheme N itself does not have an unstable steady state for any choice of parameter values and hence is not oscillatory.

However, oscillation may be introduced by direct coupling of the NO_x and O_3 cycles by relating the parameter S_{O3} to [O_3] and [NO_x] via eq 3.

$$S_{O3} = S_{O3}' + k_{N4}[O_3][NO_x]/(1 + [NO_x]) \quad (3)$$

Equation 3 allows for autocatalytic growth of O_3 (positive feedback involving O_3, NO_x, HO_x, and CO), as discussed in section 5, but brakes O_3 production at either low [O_3] or low [NO_x]. The (1 + [NO_x]) term in the denominator causes the accelerating influence of increasing [NO_x] to eventually diminish, mainly reflecting [HO_x] loss in R7. Oscillatory solutions generated by this model are shown in Figure 9. The NO_x-empty/refill (and corresponding HO_x-empty/refill) processes are clearly visible, along with the O_3-production/loss cycle. The numerical value of the [O_3][NO_x]/(1 + [NO_x]) term also is shown in Figure 9. We note that while [NO_x] varies only between 0.2 and 0.35 during the oscillations shown in Figure 9, leaving S_{O3} to a first approximation linear in [O_3][NO_x]; the nonlinear 1/(1 + [NO_x]) term is necessary to obtain oscillation.

8. Discussion

Three components have been identified as common to dynamic instability and oscillation in five related but increasingly complex models of tropospheric chemistry. The first of these components is an NO_x-empty/refill cycle in which [NO_x] grows or declines, depending upon the relative source rates of NO_x and HO_x, the latter of these being generally proportional to the photolysis rate of [O_3]. The second component is a complex O_3-production/loss cycle dependent upon [NO_x], [HO_x], [CO], and [O_3]. The third component is nonlinear coupling (both direct and indirect) of the first two, which allows each of the two cycles to affect the other. This coupling also introduces a positive feedback that autocatalytically accelerates O_3 production at high [CO] and [O_3] and low [NO_x], and thus apparently destabilizes the steady state. A simple model (Scheme N) provides a working schematic of these components of tropospheric oscillation and indicates that the positive feedback indeed is necessary for oscillation to occur.

The major features governing behavior of the dynamic instability and related oscillation in simpler models also are

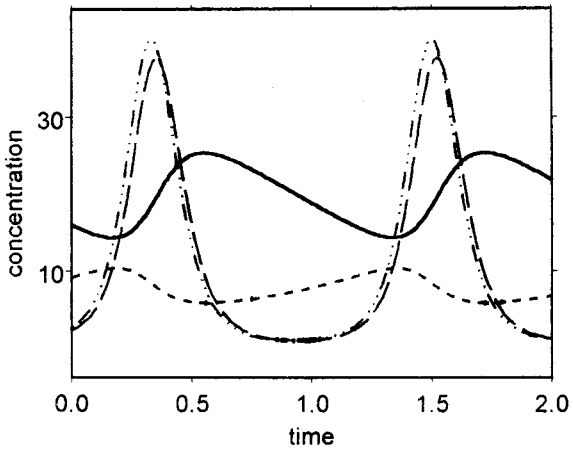

Figure 9. Dimensionless concentration oscillations versus time (dimensionless) for Scheme N. $[HO_x]$ (solid line), $[NO_x] \times 30$ (dotted line), $[O_3]$ (dashed line), and $\{[O_3][NO_x]/(1 + [NO_x])\}/20$ (dashed-dotted line). $S_{O3}' = 1$, $S_{NOx} = 20$, $k_{N1} = 4$, $k_{N2} = 4$, $k_{N3} = 1$, $k_{N4} = 100$.

dominant in a larger oscillatory model of tropospheric CH_4 photooxidation. Thus, dynamical instability and oscillation appear to be common features of both simple and more complex tropospheric chemical mechanisms, regardless of the particular reaction set or parameter values chosen. It results from complex nonlinear coupling of the NO_x-empty/refill and O_3-production/loss cycles.

While it is clear that the period of the oscillations investigated here may be too long for their simple manifestation locally in "real" atmospheres, two potential effects of the basic instability may be identified. First, while a complete oscillation may not be seen, a portion of one (e.g., a sharp change in $[O_3]$) may occur and be observed locally before being mixed into the surrounding meteorology. Such sharp fluctuations in chemical concentration are commonly observed and in fact often are attributed to meteorological complexity. But some may result from chemical instability. These could be identified on the basis of a signature derived from the analyses presented here, for example, by looking at the associated changes in $[NO]/[NO_2]$ and $[NO_x]/[CO]$. Thus, while the characteristics of high- and low-$[NO_x]$ states and chemistry are well known,[14−19] the nature of transitions between these states, as is described here, has previously not been as well understood. We believe that the focus that develops here on the role in net O_3 production of the ratio $[NO]/[NO_2]$ within $[NO_x]$ during these transitions is of particular importance. These insights are likely to be useful in separating chemical and meteorological effects in real atmospheres.

Second, the dynamical instability itself may be significant. A simple steady state is seldom attained in a real atmosphere due to meteorology, changing parameters, and varying solar flux. However, the stability of the underlying chemical steady state does influence the system, because it determines the direction of evolution of the current state. Furthermore, stability of such steady states adds stability to both the troposphere itself and to simulations of it. If an atmospheric state enters a region of parameter space where its evolution is influenced not by a stable steady state but by a dynamic instability (such as a limit cycle or a bistable regime), then its further evolution may become very difficult to predict. Thus, small changes in parameter values or initial conditions may result in significantly different trajectories as the variables track different phases of oscillation or gravitate toward one bistable solution as opposed to another. Indeed, even deterministic chaos has been observed in model M1.[6]

Acknowledgment. This work was supported by the National Science Foundation under grant ATM-9819295 and by The University of Montana.

References and Notes

(1) *Oscillations and Traveling Waves in Chemical* Systems; Field, R. J., Burger, M. Eds.; John Wiley & Sons: New York, 1985.
(2) Field, R. J.; Schneider, F. W. *J. Chem. Educ.* **1989**, *66*, 195.
(3) Gray, P.; Scott, S. K. *Chemical Oscillation and Instabilities: Nonlinear Chemical Dynamics*; Oxford Science Publications: Oxford, 1990.
(4) Epstein, I. R.; Pojman, J. A. *An Introduction to Nonlinear Chemical Dynamics: Oscillations, Waves, Patterns, and Chaos*; Oxford University Press: New York, 1998.
(5) Field, R. J.; Györgyi, L. Eds. *Chaos in Chemistry and Biochemistry*; World Scientific: Singapore, 1993.
(6) Field, R. J.; Hess, P. G.; Kalachev, L. V.; Madronich, S. *J. Geophys. Res.* **2001**, *106D*, 7553.
(7) Madronich, S.; Hess, P. G. In *Physico-Chemical Behaviour of Atmospheric Pollutants*, Proceedings of the Sixth European Symposium, Varese, Italy, 18−22 October, 1993; Angeletti, G., Restelli, G., Eds.; Rep. EUR 15609/1 EN, Office for Official Publications of the European Community: Luxembourg, 1994; pp. 5−13.
(8) Stewart, R. W. *J. Geophys. Res.* **1995**, *100D*, 8929.
(9) Krol, M. C. *J. Geophys. Res.* **1995**, *100D*, 11, 699.
(10) Poppe, D.; Lustfeld, H. *J. Geophys. Res.* **1996**, *101D*, 14373.
(11) Hess, P. G.; Madronich, S. *J. Geophys. Res.* **1997**, *102D*, 15949.
(12) Krol, M.; Poppe, D. *J. Atmos. Chem.* **1998**, *29*, 1.
(13) Konovalov, I. B.; Feigin, A. M.; Kulikov, M. Y.; Mazur, A. B. *Nonlinear Dynamic Properties of the Photochemical System of the Atmospheric Boundary Layer Under Polluted Conditions*; Preprint No. 527, Russian Academy of Sciences, Institute of Applied Physics: Nizhny Novogorod, 2000.
(14) Kleinman, L. I. *J. Geophys. Res.* **1991**, *96D*, 20721.
(15) Stewart, R. W. *J. Geophys. Res.* **1993**, *98D*, 20601.
(16) Kleinman, L. I. *J. Geophys. Res.* **1994**, *99D*, 16831.
(17) Kalachev, L. V.; Field, R. J. *Geophys. Res. Lett.* **1998**, *25*, 4505.
(18) Sillman, S. *Atmos. Environ.* **1999**, *33*, 1821.
(19) Mason, S. A.; Field, R. J.; Yokelson, R. J.; Kochivar, M.; Tinsley, M. R.; Ward, D. E.; Hao, W.-M. *J. Geophys. Res.* **2001**, *106D*, 12527.
(20) Ryerson, T. B.; Trainer, M.; Holloway, J. S.; Parrish, D. D.; Huey, L. G.; Sueper, D. T.; Frost, G. J.; Donelly, S. G.; Schauffer, S.; Atlas, E. L.; Kuster, W. C.; Golden, P. D.; Hübler, G.; Meagher, J. F.; Fehsenfeld, F. C. *Science* **2001**, *292*, 719.
(21) Sonnemann, G.; Fichtelmann, B. *J. Geophys. Res.* **1997**, *102D*, 1193.
(22) Johnson, B. R.; Scott, S. K.; Tinsley, M. R. *J. Chem. Soc., Faraday Trans.* **1998**, *94*, 2709.
(23) Sonneman, G.; Feigin, A. M. *Phys. Rev. E* **1999**, *59*, 1719.
(24) Field, R. J.; Tinsley, M. R., work in progress.
(25) Mauzerall, D. L.; Jacob, D. J.; Fan, S.-M.; Bradshaw, J. D.; Gregory, G. L.; Sachse, G. W.; Blake, D. R. *J. Geophys. Res.* **1996**, *101D*, 4175.
(26) Castro, T.; Madronich, S.; Rivale, S.; Muhlia, A.; Mar, B. *Atmos. Environ.* **2001**, *5*, 1765.
(27) O'Brien, S. R.; Mayewski, P. A.; Meeker, L. D.; Meese, D. A.; Twickler, M. S.; Whitlow, S. I. *Science* **1995**, *270*, 1962.
(28) Tinsley, M. R.; Field, R. J. *Geophys. Res. Lett.* **2001**, *28*, 4437.
(29) Berge, E.; Huang, H.-C.; Chang, J.; Liu, T.-H. *J. Geophys. Res.* **2001**, *106D*, 1347.
(30) Crutzen, P. J. *Faraday Discuss.* **1995**, *100*, 1.
(31) Johnston, H.; Kinnison, D. *J. Geophys. Res.* **1998**, *103D*, 21967.
(32) Madronich, S.; Hess, P.; Fischer, C. *NCAR Rep*, *NCAR 90−8*; National Center for Atmospheric Research: Boulder, CO, 1993.
(33) Madronich, S.; Calvert, J. G. *NCAR Tech. Note*, *NCAR TN-333-STR*; National Center for Atmospheric Research: Boulder, CO, 1989.